DOI: 10.1002/ejic.200600286

Galactose Oxidase Models: Creation and Modification of Proton Transfer Coupled to Copper(II) Coordination Processes in Pro-Phenoxyl Ligands

Fabien Michel,[a] Fabrice Thomas,*[a] Sylvain Hamman,[a] Christian Philouze,[a] Eric Saint-Aman,[b] and Jean-Louis Pierre[a]

Keywords: Copper / Phenoxyl / Tripodal ligands / Proton transfer / Radicals

Two tripodal ligands containing two pyridyl and one 4-(benzimidazol-2-yl)-2-*tert*-butylphenol (HL^H) and one 2-*tert*-butyl-4-(*N*-methylbenzimidazol-2-yl)phenol (HL^{Me}) unit have been synthesized. They possess a N_3O donor set that is known to stabilize phenoxyl radicals more efficiently than the corresponding N_2O_2 donor unit. Reaction of one molar equiv. of $Cu(ClO_4)_2{\cdot}6H_2O$ with HL^H or HL^{Me} affords the zwitterionic benzimidazolium phenolate complexes $[Cu^{II}(HL^H)]^{2+}$ and $[Cu^{II}(HL^{Me})]^{2+}$ via a proton transfer reaction coupled to copper(II) coordination. Addition of $HClO_4$ to $[Cu^{II}(HL^H)]^{2+}$ and $[Cu^{II}(HL^{Me})]^{2+}$ results in the formation of the benzimidazolium phenol complexes $[Cu^{II}(H_2L^H)]^{3+}$ and $[Cu^{II}(H_2L^{Me})]^{2+}$, while addition of NEt_3 affords the benzimidazol-phenolate complexes $[Cu^{II}(L^H)]^{2+}$ and $[Cu^{II}(L^{Me})]^{2+}$, respectively. The phenol's pK_a is remarkably low due to the strong withdrawing effect of the benzimidazolium substituent. X-ray crystallographic analysis of the copper(II) complexes shows that deprotonation of the axial phenol forces the metal to move out of the square plane towards the oxygen atom, and one (or two) $Cu–N_{pyridine}$ equatorial bond length increases. The copper(II) phenoxyl species $[Cu^{II}(HL^H)]^{\cdot 3+}$ and $[Cu^{II}(HL^{Me})]^{\cdot 3+}$ were prepared electrochemically, or by addition of two molar equiv. of copper(II) to HL^H or HL^{Me}. Under these conditions, radical formation has never been observed for tripodal ligands containing two pyridyl and one 2,4-di-*tert*-butylphenol group. This difference is explained in terms of the proton transfer mechanism and redox potentials.

Introduction

Galactose Oxidase (GO) is a copper(II) enzyme that catalyses the oxidation of primary alcohols to the corresponding aldehydes, with concomitant reduction of dioxygen to hydrogen peroxide.[1–11] This two electron chemistry is promoted by a single copper atom, working in synergy with a tyrosyl radical from the protein. Galactose Oxidase possesses a N_2O_2 donor set: One oxygen atom, from the $Tyr_{272}^{\cdot}$ radical residue, is the organic redox center, while the other (from Tyr_{495}) controls the proton transfer process. The mechanism by which the radical is generated is of major interest. It has been shown recently that mixing apo-GO with copper (I or II) in the presence of O_2 affords the Cu^{II} radical enzyme.[12–15] During the last few years, several model compounds for the GO active site have been developed.[16–48] Tripodal ligands have been widely used, and it has been shown that they are good structural models, which reproduce quite well the spectroscopic signatures of GO, and sometimes are able to model GO's reactivity towards alcohol oxidation.[17,25,27,28,35,38,41,45] It has also been shown that tripodal ligands possessing a N_3O donor set stabilize more efficiently copper(II) coordinated phenoxyl radicals than the corresponding N_2O_2 set.

We have recently developed a biomimetic approach to radical cofactor formation. In this context, we have studied the solution chemistry of several tripodal ligands,[49] involving one pro-phenoxyl group (mimicking the amino acids of the GO active site), under various copper(II), base, and dioxygen reagent conditions.[50] We have shown that Cu^{II} phenoxyl radical species could be obtained by adding two equiv. of copper(II) to ligands possessing a N_3O coordination moiety, such as HLt^{Bu} (Scheme 1), in the presence of one equiv. of triethylamine (O_2 is not involved in the reaction). In the absence of base, only a small amount of radical species is formed. In order to bypass this base requirement for radical formation, and thus to obtain more biologically relevant systems, we have synthesized the ligands HL^H and HL^{Me} (Scheme 1). Their structures are also tripodal, with two pyridyl and one phenol moiety joined together by a pivotal amino nitrogen atom. The 2-*tert*-butylphenol unit is substituted at its 4-position (with respect to the coordinating oxygen atom) by a benzimidazole (HL^H) or *N*-methylbenzimidazole (HL^{Me}) group in order to control the proton transfer processes, as do some non-coordinating histidine

[a] Laboratoire de Chimie Biomimétique, LEDSS, UMR CNRS 5616, ICMG FR CNRS 2607, Université J. Fourier, B. P. 53, 38041 Grenoble cedex 9, France
Fax: +33-4-7651-4836
E-mail: Fabrice.Thomas@ujf-grenoble.fr
[b] Pr. E. Saint-Aman, LEOPR, UMR CNRS 5630, ICMG FR CNRS 2607, Université J. Fourier, B. P. 53, 38041 Grenoble Cedex 9, France

residues in enzymes. This substituent is also known to stabilize phenoxyl radicals.[51–52] Another aspect highlighting the originality of HL^H and HL^{Me} is their ability to manage the two proton/two electron shuttle process (like GO), unlike other copper(II) complexes containing N_3O ligands. The phenoxyl oxygen atom and the copper(II) ion may control the two electron transfer, while the benzimidazolium/benzimidazole and phenol/phenoxyl acidobasic couples may be involved in the transfer of two protons. Their chemistry is therefore close to that of copper complexes of ligands possessing a N_2O_2 donor set, while their N_3O donor set is expected to enhance the stability of the phenoxyl radicals.

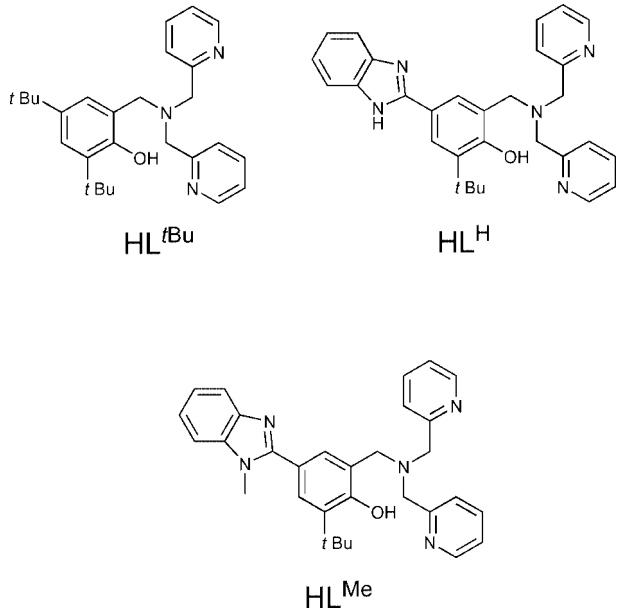

Scheme 1. Formulae for the ligands.

The coordination and solution chemistry of the copper(II) complexes of HL^H and HL^{Me} are described in this paper, and compared to that of an already published system based on the ligand HLt^{Bu} (Scheme 1).[50]

Results and Discussion

Synthesis of the Ligands

The ligands HL^H and HL^{Me} were obtained by using a Mannich reaction: In a one-pot synthesis, HL^H is obtained by mixing bis(2-pyridylmethyl)amine and 4-(1*H*-benzoimidazol-2-yl)-2-*tert*-butylphenol in the presence of one equiv. of formaldehyde. Ligand HL^{Me} is obtained by mixing bis(2-pyridylmethyl)amine and 2-*tert*-butyl-4-(1-methyl-1*H*-benzoimidazol-2-yl)phenol in the presence of one equiv. of formaldehyde.

The phenol benzimidazole (and not phenolate benzimidazolium) protonation state was confirmed by ^1H NMR ([D_6]DMSO) due to the hydroxy proton resonance (δ = 11.73 ppm and 11.76 ppm for HL^H and HL^{Me} respectively). Its structural attributes were confirmed by GHMBC and QHMQC sequences, showing ^3J correlations between the C2 carbon atom (δ = 136.9 ppm and 136.8 ppm for HL^H and HL^{Me} respectively), the *tert*-butyl protons (δ = 1.50 ppm and 1.49 ppm for HL^H and HL^{Me} respectively) and the hydroxy proton (see ESI).

Structures of the Copper(II) Complexes

The copper(II) phenolate complexes $[Cu^{II}(HL^H)]^{2+}$ and $[Cu^{II}(HL^{Me})]^{2+}$ were obtained by mixing stoichiometric amounts of the ligands and $Cu(ClO_4)_2{\cdot}6H_2O$ in acetonitrile. Dark blue single crystals were obtained on slow diffusion of di-*iso*-propyl ether into acetonitrile solutions of the complexes (Table 1). The ORTEP views of the phenolate complexes $[Cu^{II}(HL^H)]^{2+}$ and $[Cu^{II}(HL^{Me})]^{2+}$ are depicted in

Table 1. Crystallographic data for $[Cu^{II}(H_2LH)]^{3+}$, $[Cu^{II}(HLH)]^{2+}$, $[Cu^{II}(H_2LMe)]^{3+}$ and $[Cu^{II}(HLMe)]^{2+}$.

	$[Cu^{II}(H_2LH)]^{3+}$	$[Cu^{II}(HLH)]^{2+}$	$[Cu^{II}(H_2LMe)]^{3+}$	$[Cu^{II}(HLMe)]^{2+}$
Formula	$C_{34}H_{38}Cl_3CuN_7O_{13}$	$C_{36}H_{40}Cl_2CuN_8O_9$	$C_{37}H_{43}Cl_3CuN_8O_{15.33}$	$C_{35}H_{39}Cl_2CuN_7O_{9.66}$
M	922.62	863.21	1015.03	846.80
Crystal system	monoclinic	triclinic	triclinic	monoclinic
Space group	*C*2/*c*	*P*-1	*P*-1	*P*21/*n*
a [Å]	32.92(4)	8.142(2)	8.487(2)	8.460(3)
b [Å]	15.38(2)	11.656(2)	15.076(2)	22.356(4)
c [Å]	19.91(2)	21.504(4)	19.185(3)	20.324(7)
α [°]	90	96.99(2)	94.57(1)	90
β [°]	121.13(1)	95.82(2)	101.33(1)	101.5(3)
γ [°]	90	105.53(2)	100.05(1)	90
V [Å^3]	8630(16)	1932.4(8)	2353.3(8)	3766(1)
Z	8	2	2	4
T [K]	150	150	150	150
D_c [g cm^{-3}]	1.420	1.483	1.432	1.493
μ [cm^{-1}]	0.758	0.768	0.707	0.787
Monochromator	graphite	graphite	graphite	graphite
Wavelength	Mo-K_α (0.71073 Å)	Mo-K_α (0.71073 Å)	Mo-K_α (0.71073 Å)	Mo-K_α (0.71073 Å)
Reflections collected	47630	48235	40692	27910
Independent reflections (R_{int})	11386 (0.10131)	11277 (0.08692)	7530 (0.11620)	6410 (0.09244)
Observed reflections	11386 [$I > 2\sigma(I)$]	7923 [$I > 2\sigma(I)$]	4975 [$I > 2\sigma(I)$]	4624 [$I > 2\sigma(I)$]
R	0.0922	0.0403	0.0931	0.0887
R_w	0.1366	0.0530	0.1264	0.1310

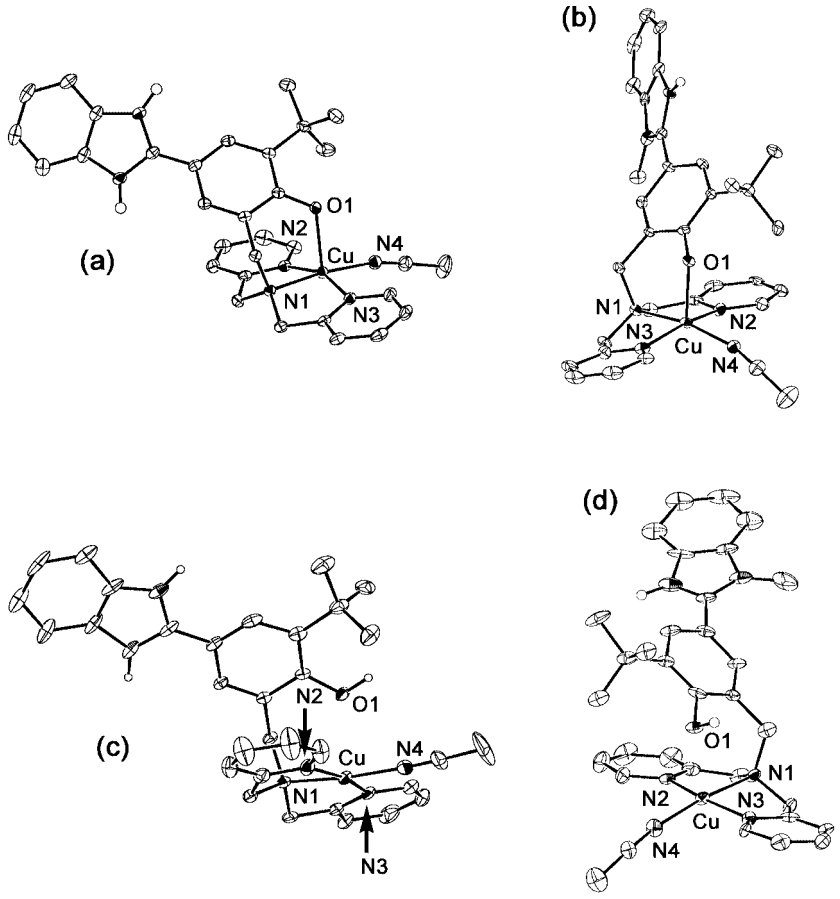

Figure 1. ORTEP view showing 35% displacement ellipsoids, and partial atomic labelling for (a) $[Cu^{II}(HL^{H})]^{2+}$, (b) $[Cu^{II}(HL^{Me})]^{3+}$, (c) $[Cu^{II}(H_2L^{H})]^{2+}$ and (d) $[Cu^{II}(H_2L^{Me})]^{3+}$. Hydrogen atoms, except the phenolic proton as well as the iminium protons, have been omitted for clarity. Weakly coordinating perchlorates are not shown (see text). Selected distances and angles are reported in Table 2.

Figure 1 (see parts a and b, respectively), and selected bond lengths and angles listed in Table 2. The geometry around the metal center is octahedral, with the copper(II) ion coordinated in a square plane by one tertiary nitrogen atom, N1, two pyridine nitrogen atoms, N2 and N3, and one acetonitrile nitrogen atom, N4. The phenolate oxygen atom, O1, occupies one axial position, and one perchlorate oxygen atom, O8, is very weakly coordinated at the opposite axial position.

In $[Cu^{II}(HL^{H})]^{2+}$ (Figure 1, a), the bond lengths are 2.021(1) Å (Cu–N1), 1.982(2) Å (Cu–N2), 1.978(1) Å (Cu–N3), 1.973(2) Å (Cu–N4), 2.156(1) Å (Cu–O1) and 2.813(2) Å (Cu–O8), while the angles N1–Cu–N2, N1–Cu–N3, N2–Cu–N4 and N3–Cu–N4 differ only slightly from 90° [83.8(1)°, 82.9(1)°, 96.2(1)° and 95.1(1)° respectively]. The mean deviation from the least square plane defined by atoms N1, N2, N3, N4, and Cu is 0.0801 Å, and the copper atom is displaced 0.205(2) Å above the basal plane towards the axial O1 oxygen atom.

In $[Cu^{II}(HL^{Me})]^{2+}$ (Figure 1, b), the Cu–N1, Cu–N2, Cu–N3, and Cu–N4 bond lengths are 2.039(5), 1.995(5), 1.999(5) and 1.981(3) Å respectively. The mean deviation from the least square plane defined by atoms N1, N2, N3, N4, and Cu is 0.036 Å. The copper atom is displaced 0.245(6) Å above the basal plane towards the axial oxygen atom, with a Cu–O1 bond length of 2.133(4) Å [the Cu–O8 distance is 2.875(5) Å].

In both $[Cu^{II}(HL^{H})]^{2+}$ and $[Cu^{II}(HL^{Me})]^{2+}$, the benzimidazolium (or *N*-methylbenzimidazolium) rings of two separate molecules, of the same complex, are π-stacked head-to-tail, with distances between the phenyl and imidazolium centroids of 3.45 and 3.53 Å for $[Cu^{II}(HL^{H})]^{2+}$ and $[Cu^{II}(HL^{Me})]^{2+}$ respectively. In both $[Cu^{II}(HL^{H})]^{2+}$ and $[Cu^{II}(HL^{Me})]^{2+}$ the iminium hydrogen atom, H1, is hydrogen bonded to the O9 oxygen atom of a perchlorate molecule.

Adding one equiv. of $HClO_4$ to acetonitrile solutions of $[Cu^{II}(HL^{H})]^{2+}$ and $[Cu^{II}(HL^{Me})]^{2+}$ affords the copper(II) phenol complexes $[Cu^{II}(H_2L^{H})]^{3+}$ and $[Cu^{II}(H_2L^{Me})]^{3+}$ that were recrystallized by diffusion of diisopropyl ether into the solution (Table 1). In $[Cu^{II}(H_2L^{H})]^{3+}$ and $[Cu^{II}(H_2L^{Me})]^{3+}$ (Figure 1, c and d, respectively) the copper(II) atoms have similar octahedral geometry. The square plane is defined by one tertiary nitrogen atom, N1, two pyridine nitrogen atoms, N2 and N3, and one acetonitrile nitrogen atom, N4. The phenolic oxygen atom, O1, and one perchlorate oxygen atom (O7 for $[Cu^{II}(H_2L^{Me})]^{3+}$ and O20 for $[Cu^{II}(H_2L^{H})]^{3+}$) occupy the apical positions.

The Cu–N1, Cu–N2 and Cu–N4 bond lengths in $[Cu^{II}(H_2L^{H})]^{3+}$ (phenol copper) are similar to those ob-

Table 2. Selected bond lengths [Å] and angles [°] for $[Cu^{II}(HL^{H})]^{2+}$, $[Cu^{II}(H_2L^{H})]^{3+}$, $[Cu^{II}(HL^{Me})]^{2+}$, $[Cu^{II}(H_2L^{Me})]^{3+}$ and $[Cu^{II}(HL^{tBu})]^{2+}$.

$[Cu^{II}(HL^{H})]^{2+}$					
Cu–N1	2.021(1)	Cu–N2	1.982(2)	Cu–N3	1.978(1)
Cu–N4	1.973(2)	Cu–O1	2.156(1)	Cu–O8	2.813(2)
N1–Cu–N2	83.77(6)	N1–Cu–N3	82.90(6)	N1–Cu–N4	172.84(6)
N2–Cu–N3	159.37(6)	N2–Cu–N4	96.18(6)	N3–Cu–N4	95.10(6)
O1–Cu–N1	93.50(5)	O1–Cu–N2	92.86(5)	O1–Cu–N3	103.60(5)
O1–Cu–N4	93.65(6)				
$[Cu^{II}(H_2L^{H})]^{3+}$					
Cu–N1	2.021(5)	Cu–N2	1.980(6)	Cu–N3	1.964(5)
Cu–N4	1.972(6)	Cu–O1	2.509(5)	Cu–O20	2.432(6)
N1–Cu–N2	83.4(2)	N1–Cu–N3	82.8(2)	N1–Cu–N4	174.9(2)
N2–Cu–N3	165.7(2)	N2–Cu–N4	96.6(2)	N3–Cu–N4	97.5(3)
$[Cu^{II}(HL^{Me})]^{2+}$					
Cu–N1	2.039(5)	Cu–N2	1.995(5)	Cu–N3	1.999(5)
Cu–N4	1.981(6)	Cu–O1	2.133(4)	Cu–O8	2.875(5)
N1–Cu–N2	84.6(2)	Cu–N3	82.5(2)	N1–Cu–N4	167.9(2)
N2–Cu–N3	160.2(2)	N2–Cu–N4	95.9(2)	N3–Cu–N4	93.7(2)
O1–Cu–N1	94.2(2)	O1–Cu–N2	96.1(2)	O1–Cu–N3	99.7(2)
O1–Cu–N4	97.8(2)				
$[Cu^{II}(H_2L^{Me})]^{3+}$					
Cu–N1	2.031(5)	Cu–N2	1.967(6)	Cu–N3	1.972(6)
Cu–N4	1.984(5)	Cu–O1	2.401(5)	Cu–O7	2.714(7)
N1–Cu–N2	83.6(2)	N1–Cu–N3	83.2(2)	N1–Cu–N4	172.3(2)
N2–Cu–N3	165.6(2)	N2–Cu–N4	97.6(2)	N3–Cu–N4	94.8(2)
$[Cu^{II}(HL^{tBu})]^{2+}$					
Cu–N1	2.037(4)	Cu–N2	1.987(4)	Cu–N3	1.977(4)
Cu–N4	1.974(6)	Cu–O1	2.456(3)		
N1–Cu–N2	83.4(2)	N1–Cu–N3	83.6(2)	N1–Cu–N4	178.5(2)
N2–Cu–N3	164.4(2)	N2–Cu–N4	95.4(2)	N3–Cu–N4	97.4(2)

served for $[Cu^{II}(HL^{H})]^{2+}$ (phenolate copper). This is not the case for the Cu–N3 bond length that is 1.964(5) Å for $[Cu^{II}(H_2L^{H})]^{3+}$, which is 0.015 Å shorter than in $[Cu^{II}(HL^{H})]^{2+}$ [1.978(1) Å]. One can also notice that the Cu–O1 bond length in $[Cu^{II}(H_2L^{H})]^{3+}$ is much longer than in $[Cu^{II}(HL^{H})]^{2+}$, it is 2.509(5) Å in $[Cu^{II}(H_2L^{H})]^{3+}$ but only 2.156(1) Å in $[Cu^{II}(HL^{H})]^{2+}$. The $Cu–O_{perchlorate}$ distance in $[Cu^{II}(H_2L^{H})]^{3+}$ [Cu–O20, 2.432(6) Å] is shorter than observed in $[Cu^{II}(HL^{Me})]^{2+}$ [Cu–O8, 2.813(2) Å].

Even more marked geometric variations, were observed for $[Cu^{II}(H_2L^{Me})]^{3+}$. The Cu–N1 and Cu–N4 bond lengths in $[Cu^{II}(H_2L^{Me})]^{3+}$ are similar to those observed in $[Cu^{II}(HL^{Me})]^{2+}$, while both the Cu–N2 and Cu–N3 bond lengths are 0.02 Å shorter (1.967(6) and 1.972(6) Å, respectively for $[Cu^{II}(H_2L^{Me})]^{3+}$, 1.995(5) and 1.999(5) Å, respectively for $[Cu^{II}(HL^{Me})]^{2+}$). The Cu–O1 bond length in $[Cu^{II}(H_2L^{Me})]^{3+}$ is significantly longer than in $[Cu^{II}(HL^{Me})]^{2+}$ (2.401(5) Å in $[Cu^{II}(H_2L^{Me})]^{3+}$, 2.133(4) Å in $[Cu^{II}(HL^{Me})]^{2+}$). The copper(II) atom is less displaced above the mean basal plane towards the axial oxygen atom in $[Cu^{II}(H_2L^{Me})]^{3+}$ [0.121(7) Å] than in $[Cu^{II}(HL^{Me})]^{2+}$ [0.245(6) Å]. The Cu–O7 distance in $[Cu^{II}(H_2L^{Me})]^{3+}$ [2.714(7) Å] is shorter than observed in $[Cu^{II}(HL^{Me})]^{2+}$. A weak π-stacking interaction (rings are slightly eclipsed) exists between the phenol unit and the imidazole ring of $[Cu^{II}(H_2L^{H})]^{3+}$, and between the *N*-methylbenzimidazolium rings of two $[Cu^{II}(H_2L^{Me})]^{3+}$ complexes, the rings are stacked head-to-tail, as in $[Cu^{II}(HL^{Me})]^{2+}$. Hydrogen bonds are present between the two iminium hydrogen atoms, H2 and H3, of $[Cu^{II}(H_2L^{H})]^{3+}$ and the perchlorate oxygen atoms, O4 and O14. One hydrogen bond is present between the iminium hydrogen atom, H2, of $[Cu^{II}(H_2L^{Me})]^{3+}$ and the perchlorate oxygen atom, O15, while another is present between the phenolic proton, H1, and the oxygen atom, O2, of one perchlorate molecule.

In these structures, another important point of note is the torsion angle between the phenol(ate) and the *para* substituent of the ring. It is significantly higher for the *N*-methylbenzimidazole (40° and 35° for $[Cu^{II}(H_2L^{Me})]^{3+}$ and $[Cu^{II}(HL^{Me})]^{2+}$, respectively) than for the benzimidazole (4° and 27° for $[Cu^{II}(H_2L^{H})]^{3+}$ and $[Cu^{II}(HL^{H})]^{2+}$, respectively), this may be explained, at least partially, by consideration of the steric hindrance of the methyl group. The consequence of this difference will be weaker electronic communication between the groups in the former case.

Complexes $[Cu^{II}(HL^{H})]^{2+}$ and $[Cu^{II}(HL^{Me})]^{2+}$ belong to the small class of structurally characterized mononuclear copper(II) complexes of tripodal ligands, in which the phenolate group occupies the unusual axial position. The complexes that belong to this class usually involve only one coordinating phenolate, and exhibit a relatively long Cu–O bond (higher than 2.17 Å).[24] In $[Cu^{II}(HL^{H})]^{2+}$, and espe-

cially in $[Cu^{II}(HL^{Me})]^{2+}$, the Cu–O1 distances are shorter [2.156(1) and 2.133(4) Å, respectively], making them the shortest bonds reported for axially coordinated phenolates.

We have previously reported the X-ray crystal structures of both the copper(II) phenol and the copper(II) phenolate complexes of HL^{NO2}, the structures of which are related to HL^{H} (they bear a nitro instead of a benzimidazole substituent).[49] Unfortunately, the exogenous ligand was different in these structures, an acetonitrile molecule in the phenol form, and a chloride ion in the phenolate form. Thus, the influence of the protonation of the axial phenolate on the equatorial bonds could not be visualized. Here, we report X-ray structures in which the phenolate and phenol forms have been crystallized with the same exogenous ligand (acetonitrile molecule) coordinated to the metal center. To the best of our knowledge, this is the first example in which changes in the copper(II) ion geometry, induced by deprotonation of the axial phenol, could be visualized so clearly: the metal moves out of the basal plane towards the oxygen atom as a consequence of a stronger axial bond, and one (or both) Cu–$N_{pyridine}$ bond length(s) increase, reflecting the weakening of the equatorial bonds (Figure 2).

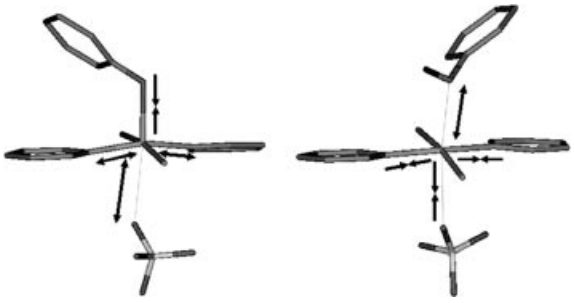

Figure 2. Influence of the phenol protonation state on the Cu–O and Cu–N bond lengths in $[Cu^{II}(HL^{Me})]^{2+}$ (left) and $[Cu^{II}(H_2L^{Me})]^{3+}$ (right).

Spectroscopic Properties of the Copper(II) Complexes

The electronic spectra of acetonitrile solutions of $[Cu^{II}(H_2L^{H})]^{3+}$ and $[Cu^{II}(H_2L^{Me})]^{3+}$ show d-d transitions at around 600 nm (Table 3, Figure 3). This suggests that the phenol subunit remains protonated in solution, and that the copper(II) atom resides within an octahedral (with a very weakly coordinated perchlorate) or square pyramidal coordination sphere (without the perchlorate). The EPR spectra of frozen CH_3CN solutions of $[Cu^{II}(H_2L^{H})]^{3+}$ and $[Cu^{II}(H_2L^{Me})]^{3+}$ are typical of axial mononuclear copper(II) complexes, and similar to that of $[Cu^{II}(HL^{tBu})]^{2+}$ (Table 4).[49] In all three complexes, the copper(II) atoms have roughly similar geometry, in agreement with the X-ray diffraction analysis. The influence of the phenol *para* substituent cannot be visualized in the EPR spectra, as a consequence of the very weak phenolic oxygen–copper(II) bond (see above). Complexes $[Cu^{II}(HL^{H})]^{2+}$ and $[Cu^{II}(HL^{Me})]^{2+}$ exhibit, in their electronic spectra, the phenolate-to-copper(II) CT transition centered at 524 and 508 nm, respectively (Figure 3, Table 3). The low energy tail in the 700–900 nm region originates from d-d transitions. On addition of one equiv. of NEt_3 to CH_3CN solutions of

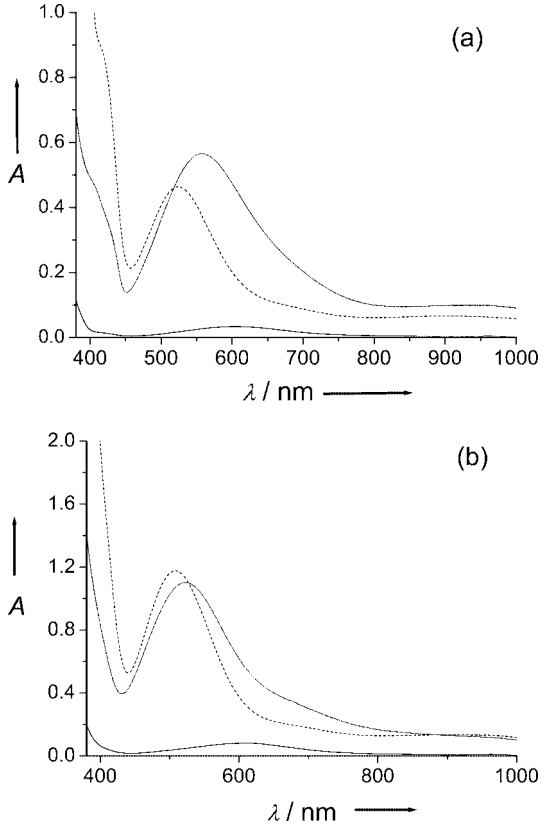

Figure 3. 298 K electronic spectra of CH_3CN solutions of: (a) 0.1 mM $[Cu^{II}(H_2L^{H})]^{3+}$ (solid line), $[Cu^{II}(HL^{H})]^{2+}$ (dashed line) and $[Cu^{II}(L^{H})]^{+}$ (dotted line); (b) 0.2 mM $[Cu^{II}(H_2L^{Me})]^{3+}$ (solid line), $[Cu^{II}(HL^{Me})]^{2+}$ (dashed line) and $[Cu^{II}(L^{Me})]^{+}$ (dotted line).

Table 3. Electronic and electrochemical properties of the copper(II) complexes in CH_3CN solutions.[a]

Complex	λ_{max} (nm) [ε ($M^{-1}cm^{-1}$)]	$E_{1/2}$[a]
$[Cu^{II}(H_2L^{H})]^{3+}$	601 br [85]	1.01[b]
$[Cu^{II}(HL^{H})]^{2+}$	415 sh [2240], 524 [1160], 700 sh [220], 900 br [165]	0.50[c]
$[Cu^{II}(L^{H})]^{+}$	405 sh [1180], 556 [1415], 700 sh [510], 900 br [245]	0.23
$[Cu^{II}(H_2L^{Me})]^{3+}$	615 br [85]	0.95[b]
$[Cu^{II}(HL^{Me})]^{2+}$	508 [1180], 664 sh [210], 900 br [135]	0.60
$[Cu^{II}(L^{Me})]^{+}$	521 [1100], 682 sh [340], 900 br [135]	0.31
$[Cu^{II}(HL^{tBu})]^{2+}$	600 [180]	>0.8[b,d]
$[Cu^{II}(L^{tBu})]^{+}$	553 [935], 950 br [180]	0.15

[a] V vs. Fc/Fc^{+}. [b] Irreversible, the value given is E_p^a. [c] Shoulder. [d] Taken from ref.[49].

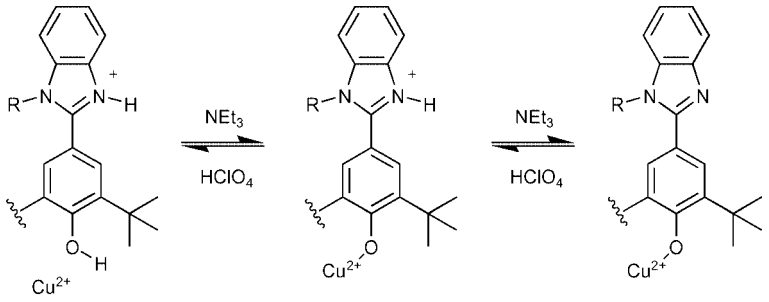

R = Me	$[Cu^{II}(H_2L^{Me})]^{3+}$	$[Cu^{II}(HL^{Me})]^{2+}$	$[Cu^{II}(L^{Me})]^{+}$
R = H	$[Cu^{II}(H_2L^{H})]^{3+}$	$[Cu^{II}(HL^{H})]^{2+}$	$[Cu^{II}(L^{H})]^{+}$

Scheme 2. Protonation equilibria for $[Cu^{II}(HL^{Me})]^{2+}$ and $[Cu^{II}(HL^{H})]^{2+}$.

$[Cu^{II}(HL^{H})]^{2+}$ and $[Cu^{II}(HL^{Me})]^{2+}$ the phenolate-to-copper(II) CT transition is displaced towards lower energy regions (556 nm and 521 nm, respectively). Such a shift can be explained by the increased donor ability of the *p*-phenolate substituent, and the subsequent deprotonation of the *N*-methylbenzimidazolium and benzimidazolium groups by NEt_3, affording the phenolate benzimidazole complexes $[Cu^{II}(L^{H})]^{+}$ and $[Cu^{II}(L^{Me})]^{+}$. Both the phenolate benzimidazolium and phenolate benzimidazole forms exhibit, in their EPR spectra, a signal typical of mononuclear copper(II) complexes (Table 4). The phenolate oxygen atom does not bridge two copper atoms (as observed when the phenolate *ortho* substituent is not sufficiently sterically hindered). The protonation equilibria involving $[Cu^{II}(HL^{H})]^{2+}$ and $[Cu^{II}(HL^{Me})]^{2+}$ are summarized in Scheme 2.

Table 4. EPR parameters of the copper(II) complexes of HL^{Me} and HL^{H} in CH_3CN at 100 K.

	$g_{xx} = g_{yy}$	g_{zz}	A_{xx}[a]	A_{yy}[a]	A_{zz}[a]
$[Cu^{II}(L^{Me})]^{+}$	2.083	2.248	0.5	0.5	17.2
$[Cu^{II}(HL^{Me})]^{2+}$	2.067	2.240	0.5	0.5	17.2
$[Cu^{II}(H_2L^{Me})]^{3+}$	2.060	2.229	1	1	18.4
$[Cu^{II}(L^{H})]^{+}$	broad				
$[Cu^{II}(HL^{H})]^{2+}$	2.056	2.235	1/1.5	1.5	18.0
$[Cu^{II}(H_2L^{H})]^{3+}$	2.060	2.233	1/1.5	1.5	18.0

[a] Values in mT.

Protonation Constants of the Complexes

The protonation constants were determined from pH-metric titrations that were monitored by UV/Vis spectroscopy (Figure 4). After dissolution of single crystals of $[Cu^{II}(H_2L^{H})]^{3+}$ and $[Cu^{II}(H_2L^{Me})]^{3+}$ into a CH_3CN/H_2O (1:1) mixture (the complexes are poorly soluble in pure H_2O), the $^{s}_{w}$pH was increased by addition of NaOH. The thermodynamic constants were obtained from refinement of the UV/Vis data by the commercial SPECFIT 32 software (Spectrum Software Associated). Their calculation was based on the spectral changes induced by addition of base. At $^{s}_{w}$pH = 2, the visible spectra of both complexes consist of Cu^{II} d-d transitions at around 650 nm ($\varepsilon < 100\ M^{-1}\,cm^{-1}$), consistent with the phenol benzimidazolium complexes being the major species present at this $^{s}_{w}$pH. The shift of the λ_{max} band that occurs when CH_3CN is replaced by CH_3CN/H_2O (1:1) suggests that the coordinating acetonitrile in $[Cu^{II}(H_2L^{H})]^{3+}$ and $[Cu^{II}(H_2L^{Me})]^{3+}$ is replaced by a water molecule from the solvent mixture. Increasing the $^{s}_{w}$pH to 5 results in the appearance of a phenolate-to-copper(II) CT in the 475–500 nm region, showing that the phenolate benzimidazolium complexes are formed. The first pK_a values, 3.40 ± 0.01 and 3.55 ± 0.02 for the copper(II) complexes of HL^{H} and HL^{Me} respectively, are thus attributed to the deprotonation of the phenol group. Such values are remarkable, as they are much lower than those reported

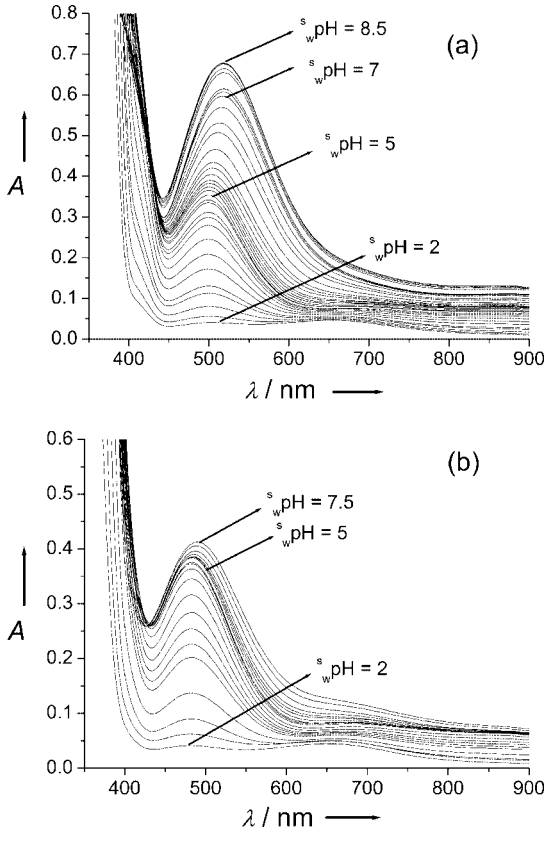

Figure 4. $^{s}_{w}$pH dependence of the electronic spectra of 0.1 mM CH_3CN/H_2O (1:1) solutions of $[Cu^{II}(H_2L^{H})]^{3+}$ (a) and $[Cu^{II}(H_2L^{Me})]^{3+}$ (b). $^{s}_{w}$pH was increased by addition of NaOH, T = 298 K, l = 1.000 cm, I = 0.1 M ($NaClO_4$).

for phenol copper(II) complexes of tripodal ligands (6.66–7.31),[50] and for GO itself (7.9).[53] This can be explained by the strong electron-withdrawing effect of the benzimidazolium (or *N*-methylbenzimidazolium) substituent that very efficiently stabilizes the phenolate form, and therefore lowers its pK_a. As a consequence, deprotonation of the phenol group occurs prior to deprotonation of the coordinated water molecule. This is in contrast with GO, for which deprotonation of the tyrosine occurs after deprotonation of the coordinated water molecule (in the absence of substrate). When the $^{s}_{w}$pH is raised to 7.5, a shift of the LMCT transition towards lower energy regions is observed, while the ε value increases by a factor of 1.7 for the copper(II) complex of HL^H, and a factor of 1.1 for the HL^{Me} complex. This structural evolution is close to that observed during addition of NEt_3 to neat acetonitrile solutions of $[Cu^{II}(HL^H)]^{2+}$ and $[Cu^{II}(HL^{Me})]^{2+}$. We therefore attribute these spectral changes to deprotonation of the benzimidazolium (or *N*-methylbenzimidazolium) group, rather than deprotonation of a coordinated water molecule. The corresponding deprotonation constants, 6.56 ± 0.02 for the copper(II) complex of HL^H and 6.22 ± 0.06 for the HL^{Me} complex are within the range of those reported for free benzimidazolium and *N*-methylbenzimidazolium (5.63 and 5.67 respectively).[54] Further increasing the $^{s}_{w}$pH results in the precipitation of the copper(II) complex of HL^{Me}. A shift of the λ_{max} band is observed for the copper(II) complex of HL^H, which may be attributed to the deprotonation of a coordinated water molecule (pK_a = 8.03 ± 0.10).

Electrochemistry of the Copper(II) Complexes

The CV curves of $[Cu^{II}(H_2L^H)]^{3+}$ and $[Cu^{II}(H_2L^{Me})]^{3+}$ in CH_3CN (0.1 M TBAP) at 298 K display an oxidation wave at E_p^a = 1.01 and 0.95 V (referred to the Fc/Fc^+ system) respectively, attributed to the oxidation of the phenol moiety (Figure 5, c). It is irreversible, attesting to the primary oxidation products not being stable over the timescale of the measurement. Therefore, the redox processes will not be investigated further.

The CV curves of the phenolate complexes $[Cu^{II}(HL^H)]^{2+}$ and $[Cu^{II}(HL^{Me})]^{2+}$ in CH_3CN display quasi reversible electrochemical signals centered at $E_{1/2}$ = 0.50 V (I_p^a/I_p^c 2.5) and $E_{1/2}$ = 0.59 V vs. Fc^+/Fc (I_p^a/I_p^c = 5), respectively (Figure 5, b). Coulometric titrations reveal that one electron redox processes are occurring in both cases, suggesting that these signals correspond to the oxidation of the phenolate to give a phenoxyl radical (vide infra). The lower I_p^a/I_p^c ratio obtained for $[Cu^{II}(HL^H)]^{2+}$ suggests that its oxidation product is more stable than the oxidation product of $[Cu^{II}(HL^{Me})]^{2+}$. Resonance effects may contribute to this, as the planarity between the phenolate ring and its *para* substituent is greater for $[Cu^{II}(HL^H)]^{2+}$ than for $[Cu^{II}(HL^{Me})]^{2+}$ in the solid state. The $E_{1/2}$ values obtained for $[Cu^{II}(HL^H)]^{2+}$ and $[Cu^{II}(HL^{Me})]^{2+}$ fall within the range for related copper(II) complexes in which the phenolate *para* substituent is either NO_2 or CF_3,[49,55] namely, an electron-withdrawing group.

Complexes $[Cu^{II}(L^H)]^+$ and $[Cu^{II}(L^{Me})]^+$ exhibit, in their CV curve, oxidation waves centered at $E_{1/2}$ = 0.23 V (I_p^a/I_p^c = 1.6) and $E_{1/2}$ = 0.32 V vs. Fc^+/Fc (I_p^a/I_p^c = 3.9), respectively (Figure 5, a). As for $[Cu^{II}(HL^H)]^{2+}$ and $[Cu^{II}(HL^{Me})]^{2+}$, these signals correspond to the oxidation of the phenolate moieties to give phenoxyl radicals. The I_p^c/I_p^a ratio, as well as the $E_{1/2}$ values, obtained for the *N*-methyl- or benzimidazolyl-phenolate complexes are lower than those found for the corresponding phenolate benzimidazolium (or *N*-methylbenzimidazolium) complexes. This reflects an increase in the stability of the oxidation products of the former complexes with respect to the latter. Deprotonation of the benzimidazolium (or *N*-methylbenzimidazolium) substituent makes the group less electron-withdrawing (inductive effect), and thus easier to be oxidized. These results nicely illustrate how an external perturbation (protonation) can influence the value of the phenoxyl/phenolate redox couple.

One Electron Oxidized Copper(II) Complexes

Upon one electron electrochemical oxidation, the violet solutions of each copper(II) phenolate complexes turn blue.

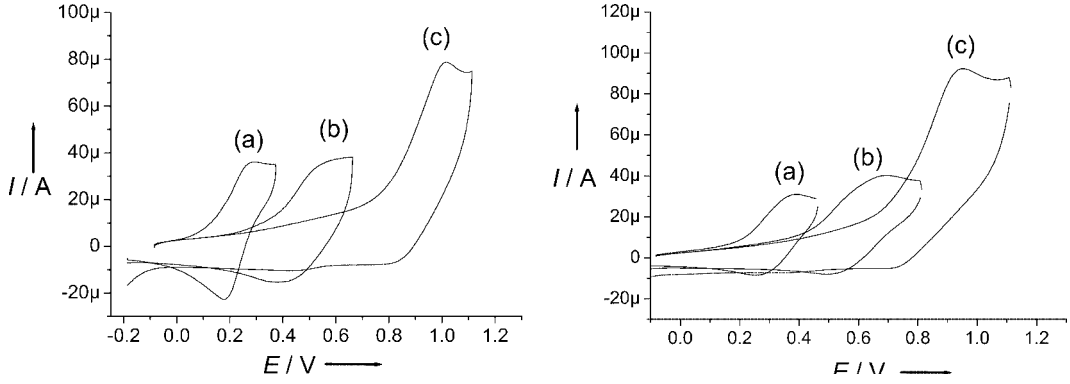

Figure 5. Cyclic voltammetry curves recorded on a vitrous carbon disc of 1 mM CH_3CN (+0.1 M TBAP) solutions of, on the left: $[Cu^{II}(L^H)]^+$ (a), $[Cu^{II}(HL^H)]^{2+}$ (b), and $[Cu^{II}(H_2L^H)]^{3+}$ (c). On the right: $[Cu^{II}(L^{Me})]^+$ (a), $[Cu^{II}(HL^{Me})]^{2+}$ (b), and $[Cu^{II}(H_2L^{Me})]^{3+}$ (c). Scan rate 0.1 V s^{-1}, T = 298 K, reference electrode Fc^+/Fc.

Two intense absorption bands at 400 and 435 nm and a lower intensity band at ca. 700 nm dominate the visible spectra, at 233 K, of the electrochemically generated $[Cu^{II}(L^{H})]^{\cdot 2+}$, $[Cu^{II}(HL^{H})]^{\cdot 3+}$ and $[Cu^{II}(HL^{Me})]^{\cdot 3+}$ complexes in CH_3CN (Figure 6 and Figure 7).[56] Such bands, which have been previously reported for copper(II) phenoxyl complexes[57–59] and $[Cu^{II}(L^{tBu})]^{\cdot 2+}$,[49] are attributed to the π-π* transitions of the radical.[60–67]

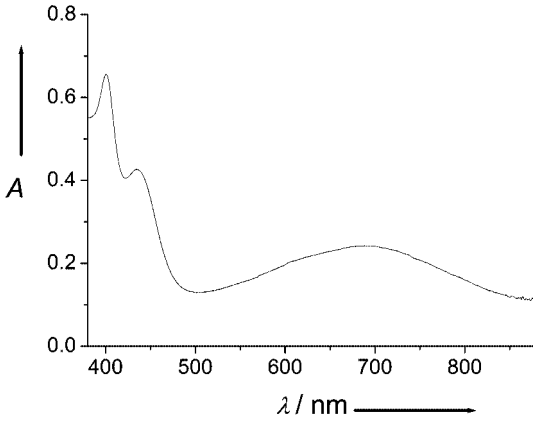

Figure 6. 233 K electronic spectra of a 0.1 mM CH_3CN solution of $[Cu^{II}(L^{H})]^{\cdot 2+}$ (l = 1.000 cm).

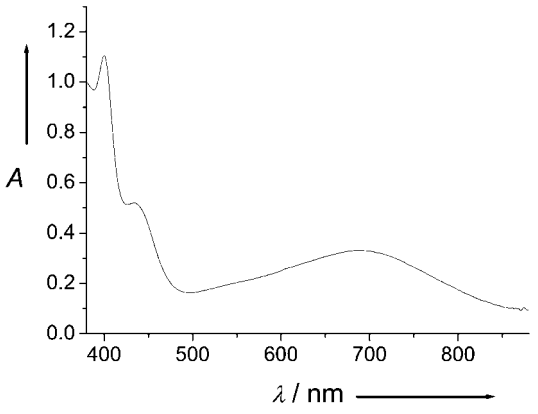

Figure 7. 233 K electronic spectra of a 0.1 mM CH_3CN solution of $[Cu^{II}(HL^{H})]^{\cdot 3+}$ (l = 1.000 cm).

The 4 K X-Band EPR spectra of the electrogenerated species $[Cu^{II}(L^{H})]^{\cdot 2+}$ and $[Cu^{II}(HL^{H})]^{\cdot 3+}$ in CH_3CN show broad $\Delta M_S = \pm 1$ transitions at 250 and 390 mT. The associated $\Delta M_S = \pm 2$ signal is seen at 150 mT. This signal is split into four hyperfine lines separated by 8 mT (Figure 8), which are attributed to the interaction of the electronic spin with the nuclear spin of the copper(II) (I = 3/2). This is clear evidence of ferromagnetic coupling between the spins of the radical and the copper(II). An additional mononuclear copper(II) signal, corresponding to degradation products, is also present in each EPR spectrum. $[Cu^{II}(L^{Me})]^{\cdot 2+}$ exhibits a weak transition at 160 mT, while $[Cu^{II}(HL^{Me})]^{\cdot 3+}$ was too unstable to be prepared in sufficient amounts to enable its EPR spectrum to be recorded.

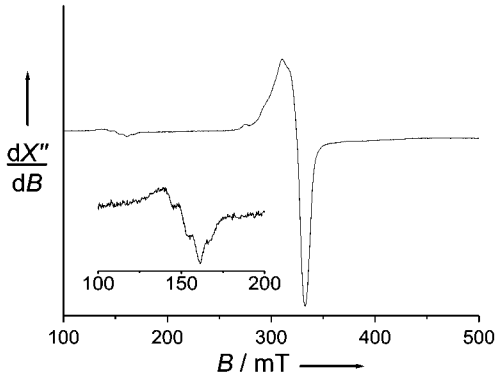

Figure 8. X-Band EPR spectra of a 1 mM CH_3CN solution of $[Cu^{II}(L^{H})]^{\cdot 2+}$. Microwave frequency 4485 GHz, power 1 mW, mod. frequency 100 kHz, amp. 1.0 mT, T = 4 K.

The temperature dependence of the UV/Vis spectrum of $[Cu^{II}(L^{Me})]^{\cdot 2+}$ precludes any investigation of its stability at 298 K, while $[Cu^{II}(HL^{Me})]^{\cdot 3+}$ was too unstable and degraded significantly even at 233 K. Complex $[Cu^{II}(L^{H})]^{\cdot 2+}$ has a decomposition rate constant k_{decay} of 0.067 min^{-1} ($t_{1/2}$ = 10.4 min at 298 K). This is 2.5 times weaker than that of $[Cu^{II}(L^{tBu})]^{\cdot 2+}$ (k_{decay} = 0.155 min^{-1}), this is likely to be due to resonance stabilization in $[Cu^{II}(L^{H})]^{\cdot 2+}$. Moreover, $[Cu^{II}(L^{H})]^{+}$ exhibits an $E_{1/2}$ value (0.23 V vs. Fc^{+}/Fc) that is roughly similar to that of $[Cu^{II}(L^{F})]^{+}$ ($E_{1/2}$ = 0.20 V),[4] the structure of which differs from that of $[Cu^{II}(L^{H})]^{+}$ by the nature of phenolate *para* substituent, which is a fluorine atom. As the radical species $[Cu^{II}(L^{F})]^{\cdot 2+}$ decomposed during electrolysis at 233 K, $[Cu^{II}(L^{H})]^{\cdot 2+}$ it should be, in principle, too unstable to be characterized. This is not true, showing that charge delocalization over the benzimidazolium group contributes significantly to the chemical stability of the radical species $[Cu^{II}(L^{H})]^{\cdot 2+}$. This also shows that the usual correlation between the chemical stability of copper(II) phenoxyl radical species, and the potential values of the phenoxyl/phenolate redox couple, is not so evident when charge delocalization occurs. Complex $[Cu^{II}(HL^{H})]^{\cdot 3+}$ was much less stable than $[Cu^{II}(L^{H})]^{\cdot 2+}$ (k_{decay} = 0.99 min^{-1}, $t_{1/2}$ = 0.7 min at 298 K), this is in agreement with the spectroscopic and electrochemical data. Protonation of benzimidazole, to produce a positively charged benzimidazolium group, makes it electron-withdrawing, which destabilizes the phenoxyl radical.

Copper(II) Titration: Addition of 0 to 1 Molar Equivalent

The solution chemistry of each ligand has been studied in acetonitrile by increasing the ratio of copper(II) perchlorate to HL^{H} and HL^{Me}. When one molar equiv. of copper(II) perchlorate is slowly added to an acetonitrile solution of HL^{H}, an absorption band appears gradually in the visible spectra at 526 nm (Figure 9), and EPR reveals the formation of a mononuclear copper(II) complex. These spectroscopic features well match those reported for the isolated copper(II) phenolate benzimidazolium species $[Cu^{II}(HL^{H})]^{2+}$. Likewise, the addition of one molar equiv.

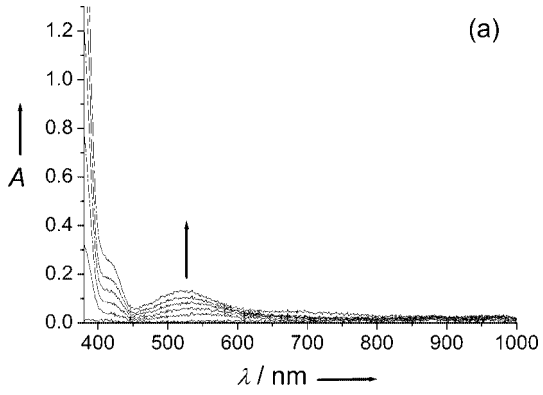

Figure 9. Titration of a 0.1 mM CH_3CN solution of HL^H against copper(II) perchlorate at 233 K: from 0 to 1 molar equiv. of copper (a), and from 1 to 2 molar equiv. of copper (b); arrows indicate spectral changes upon the addition of copper (l = 1.000 cm).

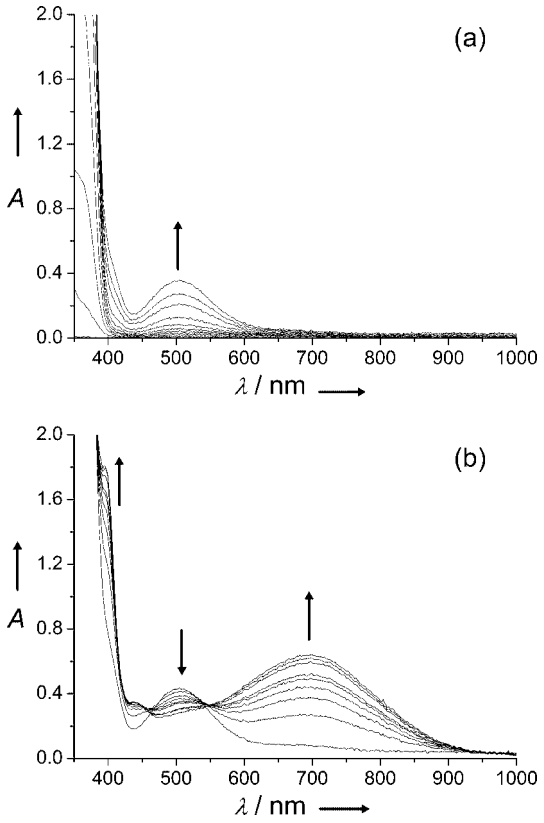

Figure 10. Titration of a 0.3 mM CH_3CN solution of HL^{Me} against copper(II) perchlorate at 233 K: from 0 to 1 molar equiv. of copper (a), and from 1 to 2 molar equiv. of copper (b); arrows indicate spectral changes upon the addition of copper (l = 1.000 cm).

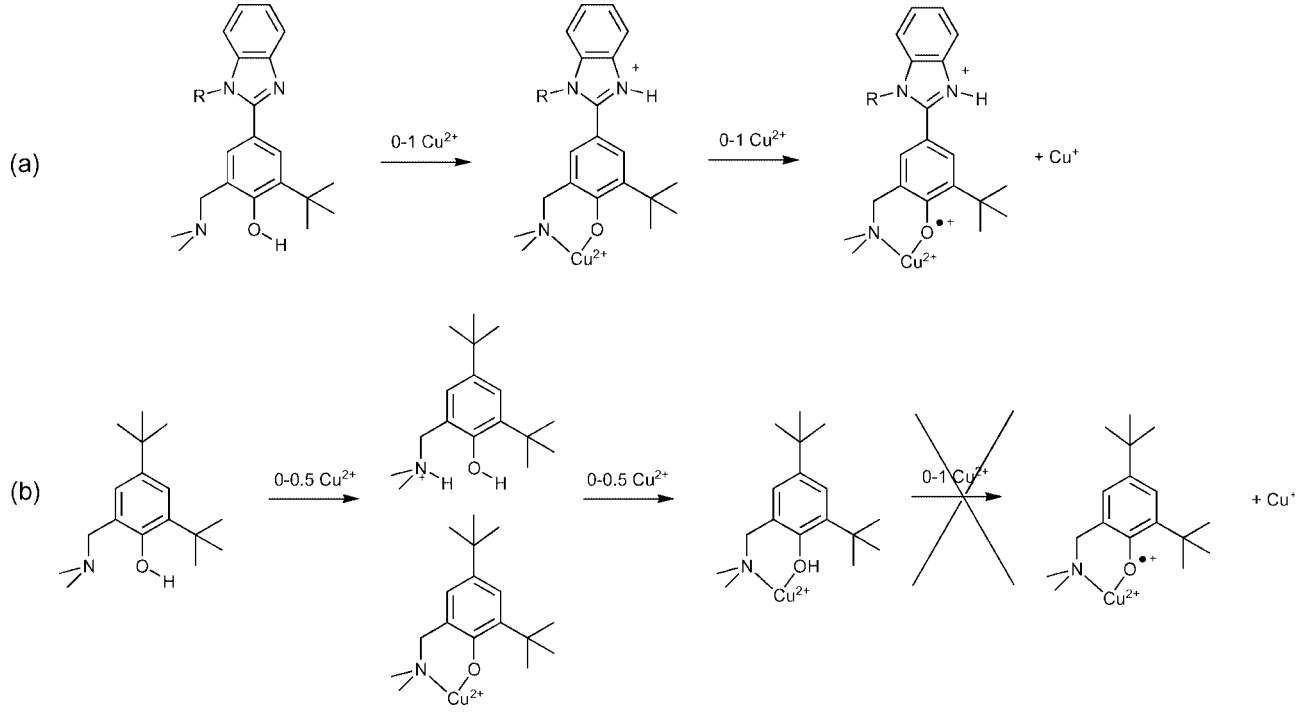

Scheme 3. Solution chemistry of HL^{Me} and HL^H (a), HL^{tBu} (b), in the presence of copper(II) perchlorate in CH_3CN.

of copper(II) to HL^{Me} affords the copper(II) phenolate *N*-methylbenzimidazolium complex $[Cu^{II}(HL^{Me})]^{2+}$ (Figure 10). Thus, the coordination of the ligands to copper(II) induces a transfer of the phenolic proton to the benzimidazole (or *N*-methylbenzimidazole) substituent (Scheme 3, a). This behavior is in sharp contrast with that of HL^{tBu} (Scheme 3, b), which after addition of one molar equiv. of copper(II) affords the copper(II) phenol complex $[Cu^{II}(HL^{tBu})]^{2+}$.[50] Moreover, formation of this phenol complex was more complicated than the simple reaction between the ligand HL^{tBu} and copper(II). As 0 to 0.5 molar equiv. of copper(II) perchlorate was added, a progressive increase in the phenolate to copper(II) CT transition was observed, showing that once the copper is chelated to by some of the available ligand in solution, the tertiary amine of the remaining free ligand deprotonates the weakly coordinated phenol (i.e. the pK_a of the coordinated phenol is lower than that of the tertiary ammonium, Scheme 3, b). When 0.5 to one molar equiv. of copper(II) is added to HL^{tBu}, the spectrum of the copper(II) phenolate complex $[Cu^{II}(L^{tBu})]^{+}$ vanishes and is replaced by that of the copper(II) phenol complex $[Cu^{II}(HL^{tBu})]^{2+}$. Complexation of copper(II) to the free protonated ligand H_2L^{tBu+} induces deprotonation of its tertiary ammonium group; the proton is transferred to the coordinated phenolate of $[Cu^{II}(L^{tBu})]^{+}$, affording the copper(II) phenol complex $[Cu^{II}(HL^{tBu})]^{2+}$ (Scheme 3, b).

Thus proton transfer, coupled to copper(II) complexation, occurs in all cases (HL^{tBu}, HL^{H} and HL^{Me}). Nevertheless, a major difference exists between HL^{tBu} and HL^{H} (and HL^{Me}) namely, the endogenous base: proton transfer is managed either by the tertiary amine of HL^{tBu}, or by the benzimidazole moiety in HL^{H} or HL^{Me}. In all these tripodal ligands, the tertiary amine is involved in copper(II) coordination. When the proton is transferred from the tertiary amine (ammonium form), it does not chelate the metal thus, a mixture of the protonated ligand and the copper(II) phenolate complex is obtained when 0.5 molar equiv. of copper(II) is added to HLt^{Bu}. The benzimidazolium group does not interfere with the complexation processes. Thus, when the proton is transferred from the benzimidazole (or *N*-methylbenzimidazole) group of HL^{H} and HL^{Me}, all of the ligand in solution chelates to the metal, and no free ligand remains, even when only 0.5 molar equiv. of copper(II) is added to the ligand. The existence, and location, of the proton acceptor in the ligand is therefore of crucial importance in dictating the mechanism by which copper(II) is chelated by tripodal ligands.

Copper(II) Titration: Addition of 1 to 2 Molar Equivalents

The acetonitrile solutions of HL^{H} and HL^{Me} were titrated against copper(II), at 233 K, and up to two molar equiv. of copper(II) was added. When one to two molar equiv. of copper(II) was added, the phenolate to copper(II) CT transition at 524 nm (and 508 nm) of $[Cu^{II}(HL^{H})]^{2+}$ (and $[Cu^{II}(HL^{Me})]^{2+}$) progressively decreases in intensity and then vanishes, while new intense transitions appear at around 400, 450 and 700 nm. The UV/Vis spectrum of the final species exhibits intense absorption bands at 401, 435 and 700 nm [396, 440 (shoulder) and 700 nm for HL^{Me}]. These features are similar to those of the electrogenerated $[Cu^{II}(HL^{H})]^{\cdot 3+}$ complex (and $[Cu^{II}(HL^{Me})]^{\cdot 3+}$). The copper(II) phenolate complexes $[Cu^{II}(HL^{H})]^{2+}$ and $[Cu^{II}(HL^{Me})]^{2+}$ are thus quantitatively oxidized by excess copper(II) to give the corresponding copper(II) phenoxyl complexes $[Cu^{II}(HL^{H})]^{\cdot 3+}$ and $[Cu^{II}(HL^{Me})]^{\cdot 3+}$, releasing free copper(I) according to Scheme 3 (a).[68]

When one molar equiv. of copper(II) was added to an acetonitrile solution of HL^{tBu}, the copper(II) phenol complex $[Cu^{II}(HL^{tBu})]^{2+}$ was obtained quantitatively. Continuing to add copper(II) results in the oxidation of a small amount of the $[Cu^{II}(HL^{tBu})]^{2+}$ complex (less than 8%) to give the radical species $[Cu^{II}(L^{tBu})]^{\cdot 2+}$, this is consistent with the oxidation potential of the phenol in $[Cu^{II}(HL^{tBu})]^{2+}$ being too high to allow it to be oxidized by copper(II) to produce the corresponding phenoxyl radical.[50]

After addition of one molar equiv. of copper(II) to HL^{H} or HL^{Me} deprotonation of the phenol occurs, induced by proton transfer to the benzimidazole or *N*-methylbenzimidazole substituent, which lowers its redox potential, making oxidation by exogenous copper(II) possible in the absence of exogenous base.[69] Deprotonation of the phenol group of HL^{tBu} does not occur in the presence of one molar equiv. of copper(II), thus preventing its oxidation by excess copper(II).

On the other hand, if free copper(II) oxidizes the copper(II) phenolate complex, then one should expect the formation of a copper(II) phenoxyl complex at a copper(II)/ligand ratio lower than 1:1. This is not the case, showing that a comproportionation reaction consumes the radical once it is formed (as in the case of GO[70] and other N_3O ligands[50]) according to Equation 1.

$$\text{copper(II) phenoxyl} + \text{copper(I)} \rightarrow 2\ \text{copper(II)}-\text{phenolate} \qquad (1)$$

Conclusion

Herein we have reported a fine structural approach to the protonation/deprotonation sequence of the axial Tyr_{495} in the GO active site. We have also provided evidence of a proton transfer reaction coupled to a copper(II) coordination process occurring in the ligands: in the presence of one molar equiv. of copper(II) the phenolic proton moves towards the *p*-benzimidazole (or *N*-methylbenzimidazole) substituent affording *p*-benzimidazolium phenolate complexes. In the presence of excess copper(II) (in absence of an exogenous base), a copper(II) phenoxyl radical is obtained, which was not observed for related ligands possessing a *p*-*tert*-butyl group. The existence and location of the proton acceptor (tertiary amine or benzimidazole) in the ligand is therefore of crucial importance in dictating the mechanism by which copper(II) is chelated, and influences the reactivity of the complex towards an exogenous oxidizer.

The control of the proton transfer and the metal coordination, are of prime importance in stabilizing phenoxyl radicals in proteins.[71–79] Recently, each phenomenon has been explored independently in biomimetic systems. This lead to the characterization of metal coordinated phenoxyl radicals,[16–50] or hydrogen bonded phenoxyl radicals generated by proton coupled to electron transfer.[80–83] Ligands HL^H and HL^{Me} are the first systems where both proton transfer and metal coordination occur simultaneously, contributing to the stabilization of the phenoxyl radical (by deprotonation, lowering of the redox potential by at least 0.35 V, metal coordination, and by resonance).

Experimental Section

General: All chemicals were of reagent grade and used without purification. Microanalyses were performed by the Service Central d'Analyses du CNRS (Lyon, France).

Low-temperature visible spectra were recorded on a CARY 50 spectrophotometer equipped with a low temperature Hellma immersion probe (1.000 cm path length quartz cell). The temperature was controlled with a Lauda RK8 KS cryostat.

X-band EPR spectra were recorded on a BRUKER ESP 300E spectrometer equipped with a BRUKER nitrogen flow cryostat, and a BRUKER EMX spectrometer equipped with an ESR 900 helium flow cryostat (Oxford Instruments). Spectra were treated using the WINEPR software and simulated using the BRUKER SIMFONIA software.

Rate constants for the self-decomposition of the radical species were obtained spectrophotometrically. The absorbance decay at 450 nm (298 K) was fitted using the Biokine software (Bio Logic Co, Claix, France).

The cyclic and differential pulse voltammograms of each compound (1 mM) in CH_3CN, containing 0.1 M tetra-*n*-butylammonium perchlorate (TBAP) as the supporting electrolyte, were recorded on a CHI potentiostat at 298 K. The working electrode was a glassy carbon disc, and the secondary electrode was a Pt wire, and the reference electrode was 0.01 M $Ag/AgNO_3$. The potential of the regular ferrocenium/ferrocene (Fc^+/Fc) redox reaction, +0.087 V under our experimental conditions, was used as an internal reference. Electrolysis was performed at 233 K at a carbon felt electrode using a PAR 273 potentiostat.

Crystal Structure Analysis: For all structures, collected reflections were corrected for Lorentz and polarization effects, but not for absorption. The structures were solved by direct methods and refined using the TEXSAN software. All non-hydrogen atoms were refined with anisotropic thermal parameters. Hydrogen atoms were generated at idealized positions, and were modeled as riding on the carrier atoms, and refined with isotropic thermal parameters.

CCDC-259962, -259841, -275709 and -275881 contain the supplementary crystallographic data for this paper. These data can be obtained free of charge from The Cambridge Crystallographic Data Centre via www.ccdc.cam.ac.uk/data_request/cif.

3-*tert*-Butyl-4-hydroxybenzaldehyde: 2-*tert*-Butylphenol (20 g, 133 mmol) was dissolved in MeOH (80 mL), NaOH (80 g) was dissolved in water (80 mL) and added dropwise to the reaction mixture. Then $CHCl_3$ was added (during the course of 1 h) at 60 °C. The reaction mixture was stirred for 3 h, then cooled to 0 °C and hydrolyzed with 4 N HCl until the solution reached pH 5–6. The mixture was extracted with $CHCl_3$ and the combined organic layers were dried with Na_2SO_4 and then concentrated. Column chromatography on silica gel [ethyl acetate:pentane (1:20) was the eluent] yielded 3-*tert*-butyl-4-hydroxybenzaldehyde (24 g, 40%) as an orange solid. ^1H NMR (200 MHz, $CDCl_3$): δ = 1.44 (s, 9 H), 6.85–6.89 [d, $^3J_{H,H}$ = 8.2 Hz, 1 H], 7.62–7.67 [dd, $^3J_{H,H}$ = 8.2 Hz, $^4J_{H,H}$ = 1.7 Hz, 1 H], 7.84–7.85 [d, $^4J_{H,H}$ = 1.7 Hz, 1 H], 9.84 ppm (s, 1 H). ^{13}C NMR (75 MHz, $CDCl_3$): δ = 29.7 (t, 3C), 35.1 (q), 117.5 (s), 129.9 (q), 130.6 (s), 137,6 (q), 161.2 (q), 192.3 ppm (s). M.p. 125 °C. $C_{11}H_{14}O_2$ (178.23): calcd. C 74.13, H 7.92; found C 73.45, H 7.85.

2-*tert*-Butyl-4-(1-methyl-1*H*-benzoimidazol-2-yl)phenol: To 3-*tert*-Butyl-4-hydroxybenzaldehyde (1.04 g, 5.8 mmol) in MeOH (20 mL) was added *N*-methyl-1,2-phenylenediamine (0.709 g, 5.8 mmol) at 0 °C. The mixture was stirred for 0.5 h at 0 °C, and then for 3 h at room temperature. Benzofuroxane (0.795 g, 5.8 mmol) was dissolved in CH_3CN (5 mL), and added to the reaction mixture at room temperature. The mixture was stirred for 12 h at 60 °C, then cooled to 0 °C, and 10% NaOH (10 mL) was added. The reaction was poured into 200 mL of water, and concentrated HCl was added to neutralize the solution. The brown precipitate was filtered, washed with cold water and $CHCl_3$, and then dried under vacuum. Yield: 50%. ^1H NMR (300 MHz, [D$_6$]DMSO): δ = 1.46 (s, 9 H), 3.89 (s, 3 H), 7.22–7.31 (m, 2 H), 7.54–7.60 (m, 2 H), 7.66–7.69 (m, 2 H), 10.00 ppm (s, 1 H). ^{13}C NMR (75 MHz, [D$_6$]DMSO): δ = 30.1 (t, 3C), 32.6 (t), 35.3 (q), 111.1 (s), 117.0 (s), 119.4 (s), 121.2 (q), 122.5 (s), 122.7 (s), 128.8 (s), 128.9 (s), 137.5 (q), 143.4 (q), 154.7 (q), 158.3 ppm (q). M.p. > 250 °C. MS (DCI, NH_3/isobutane) *m/z* (%): 280 (100) $[M+H]^+$. $C_{18}H_{20}N_2O$ (280.36): calcd. C 77.11, H 7.19, N 9.99; found C 75.40, H 7.21, N 9.76.

HL^{Me}: 2-*tert*-Butyl-4-(1-methyl-1*H*-benzoimidazol-2-yl)phenol (1.016 g, 3.6 mmol), bis(2-pyridylmethyl)amine (722 mg, 3.6 mmol) and formaldehyde (1.4 mL of a 37% aqueous solution) in EtOH/H_2O (5:1, 100 mL) were refluxed together for 12 h. The reaction mixture was then extracted with ethyl acetate, dried with Na_2SO_4 and then concentrated. Column chromatography on silica gel [ethyl acetate/methanol (9:1) + 1% isopropylamine was the eluent] yielded HL^{Me} (600 mg, 35%) as a pale orange solid. ^1H NMR (300 MHz, [D$_6$]DMSO): δ = 1.49 (s, 9 H), 3.89 (s, 3 H), 3.91 (s, 4 H), 3.95 (s, 2 H), 7.21–7.34 (m, 4 H), 7.42–7.44 (d, $^3J_{H,H}$ = 7.8 Hz, 2 H), 7.52–7.53 (d, $^4J_{H,H}$ = 2.0 Hz, 1 H), 7.56–7.60 (m, 1 H), 7.63–7.64 (d, $^4J_{H,H}$ = 2.0 Hz, 1 H), 7.65–7.68 (m, 1 H), 7.78–7.84 (m, $^3J_{H,H}$ = 4.7 Hz, $^4J_{H,H}$ = 1.7 Hz, 2 H), 8.59–8.60 (d, $^3J_{H,H}$ = 4.7 Hz, 2 H), 11.76 ppm (s, 1 H). ^{13}C NMR (75 MHz, [D$_6$]DMSO): δ = 32.6 (t), 35.4 (q), 57.2 (d), 59.2 (d), 111 (s), 119.4 (q), 120.5 (q), 122.5 (q), 122.7 (s), 123.4 (s, 2C), 124.0 (s, 2C), 128.1 (s), 129.8 (s), 136.8 (q), 137.5 (q), 137.7 (s, 2C), 149.7 (s, 2C), 154.6 (q), 158.4 ppm (q, 2C). MS (DCI, NH_3/isobutane) *m/z* (%): 492 (100) $[M+H]^+$. M.p. 150 °C. $C_{31}H_{33}N_5O$ (491.63): calcd. C 75.73, H 6.77, N 14.25; found C 75.65, H 7.01, N 14.19.

$[Cu^{II}(HL^{Me})](ClO_4)_2$: Ligand HL^{Me} (132 mg, 0.269 mmol) was dissolved in CH_3CN (10 mL) and $Cu(ClO_4)_2 \cdot 6H_2O$ (99 mg, 0.267 mmol) in CH_3CN (2 mL) was then added dropwise. The solution was stirred for 15 min and then the volume was reduced to 2 mL. Single crystals of $[Cu^{II}(HL^{Me})](ClO_4)_2$ were obtained by slow diffusion of diisopropyl ether into the CH_3CN solution (102 mg, yield: 68%). ESI MS (*m/z*): 553 $[M - H - (CH_3CN) - 2(ClO_4)]^+$. $C_{33}H_{36}Cl_2CuN_6O_9$ (795.13): calcd. C 49.85, H 4.56, N 10.57, Cu 7.99; found C 49.57, H 4.82, N 10.11, Cu 7.45.

$[Cu^{II}(H_2L^{Me})](ClO_4)_3$: Compound $[Cu^{II}(HL^{Me})](ClO_4)_2$ (23 mg, 0.029 mmol) was dissolved in CH_3CN (1 mL), and $HClO_4$ (70%, 2.4 μL) was added. The solution was stirred for 5 min. Single crys-

tals of $[Cu^{II}(H_2L^{Me})](ClO_4)_3$ were obtained by slow diffusion of isopropyl ether into the CH_3CN solution (18 mg, yield: 90%). ESI MS (*m*/*z*): 653 $[M - H - (CH_3CN) - 2(ClO_4)]^+$. $C_{33}H_{37}Cl_3CuN_6O_{13}$ (895.58): calcd. C 44.26, H 4.16, N 9.13, Cu 7.10; found C 44.18, H 4.13, N 9.13, Cu 6.88.

4-(1*H*-Benzimidazol-2-yl)-2-*tert*-butylphenol: To 3-*tert*-Butyl-4-hydroxybenzaldehyde (1.04 g, 5.8 mmol) in MeOH (20 mL) was added benzene-1,2-diamine (0.631 g, 5.8 mmol) at 0 °C. The mixture was stirred for 0.5 h at 0 °C, and then for 1 h at room temperature. Benzofuroxane (0.795 g, 5.8 mmol) was dissolved in CH_3CN (5 mL), and added dropwise (over a 10 min period) to the reaction mixture. The mixture was stirred for 2 h at 60 °C, then cooled to 0 °C and then 10% NaOH (10 mL) was added. The reaction mixture was poured into 200 mL of water and concentrated HCl was added to neutralize the solution. The brown precipitate was filtered, washed with cold water and $CHCl_3$, and then dried under vacuum. Yield: 52%. ^{1}H NMR (300 MHz, [D$_6$]DMSO): δ = 1.48 (s, 9 H), 6.95 (d, J = 8.1 Hz, 1 H), 7.17 (dd, ^3J = 5.9 Hz, ^4J = 3.2 Hz, 2 H), 7.57 (dd, ^3J = 5.7 Hz, ^4J = 3.2 Hz, 2 H), 7.87 (dd, ^3J = 8.1 Hz, ^4J = 1.5 Hz, 1 H), 8.05 (d, ^4J = 1.5 Hz, 1 H), 9.94 (s, 1 H), 12.68 ppm (s, 1 H). ^{13}C NMR (75 MHz, [D$_6$]DMSO): δ = 29.7 (t), 34.9 (C_q), 114.9 (CH), 116.8 (CH), 121.0 (C_q), 121.9 (CH), 125.6 (CH), 125.9 (CH), 136.2 (C_q), 139.7 (C_q), 152.6 (C_q), 158.2 ppm (C_q). M.p. > 250 °C. MS (DCI, NH_3/isobutane) *m*/*z* (%): 267 (100) $[M+H]^+$. $C_{17}H_{18}N_2O$ (266.34): calcd. C 76.66, H 6.81, N 10.52; found C 75.78, H 6.94, N 9.37.

HL^H: 2-*tert*-Butyl-4-(1*H*-benzoimidazol-2-yl)phenol (0.500 g, 1.88 mmol), bis(2-pyridylmethyl)amine (374 mg, 1.88 mmol) and formaldehyde (0.7 g of a 37% aqueous solution, 9.4 mmol) in EtOH/H_2O (2:1, 100 mL) were refluxed together for 12 h. The reaction mixture was then extracted with ethyl acetate, washed with a saturated NaCl aqueous solution, dried with Na_2SO_4 and then concentrated. Column chromatography on silica gel [ethyl acetate/methanol (5:1)] yielded HL^H (270 mg, 30%) as a beige solid. ^{1}H NMR (300 MHz, [D$_6$]DMSO): δ = 1.50 (s, 9 H), 3.90 (s, 4 H), 3.94 (s, 2 H), 7.19 (dd, ^3J = 5.9 Hz, ^4J = 3.2 Hz, 2 H), 7.30 (d, ^3J = 6.5 Hz, 1 H), 7.32 (d, ^3J = 7.1 Hz, 1 H), 7.41 (d, J = 7.8 Hz, 2 H), 7.50–7.62 (m, 2 H), 7.78 (td, ^3J = 7.6 Hz, ^4J = 1.6 Hz, 2 H), 7.87 (d, ^4J = 1.8 Hz, 1 H), 8.01 (d, ^4J = 1 Hz, 1 H, 8 Hz), 8.58 (d, ^3J = 4.0 Hz, 2 H), 11.73 (s, 1 H), 12.70 ppm (s, 1 H). ^{13}C NMR (75 MHz, [D$_6$]DMSO): δ = 30.3 (*t*Bu), 35.6 (C_q), 57.6 (CH_2), 59.1 (CH_2Py), 121.0 (C_q), 122.4 (CH), 123.4 (CH), 123.9 (CH), 124.5 (C_q), 125.4 (CH), 127.6 (CH), 135.9 (C_q), 137.2 (C_q), 137.7 (CH), 144.9 (C_q), 149.7 (CH), 153.0 (C_q), 158.5 (C_q), 158.8 ppm (C_q). M.p. 200 °C. MS (DCI, NH_3/isobutane) *m*/*z* (%): 478 (100) $[M+H]^+$. $C_{30}H_{31}N_5O$ (477.60): calcd. C 75.44, H 6.54, N 14.66; found C 75.16, H 6.55, N 14.50.

$[Cu^{II}(HL^H)](ClO_4)_2$: $[Cu^{II}(HL^H)](ClO_4)_2$ was obtained in a similar way to $[Cu^{II}(HL^{Me})](ClO_4)_2$ by using HL^H instead of HL^{Me} (yield: 75%). ESI MS (*m*/*z*): 539 $[M - H - (CH_3CN) - 2(ClO_4)]^+$. $C_{32}H_{34}Cl_2CuN_6O_9{\cdot}H_2O{\cdot}CH_3CN$ (781.10): calcd. C 48.61, H 4.68, N 11.67, Cu 7.56; found C 47.92, H 4.51, N 11.68, Cu 7.50.

$[Cu^{II}(H_2L^H)](ClO_4)_3$: Complex $[Cu^{II}(H_2L^H)](ClO_4)_3$ was obtained in a similar way to $[Cu^{II}(H_2L^{Me})](ClO_4)_3$ by using HL^H instead of HL^{Me} (yield: 90%). ESI MS (*m*/*z*): 539 $[M - H - (CH_3CN) - 2(ClO_4)]^+$. $C_{32}H_{35}Cl_3CuN_6O_{13}$ (881.56): calcd. C 44.16, H 4.38, N 9.36, Cu 7.08; found C 44.51, H 4.35, N 9.70, Cu 6.75.

Acknowledgments

The authors thank the Institute of Metals in Biology of Grenoble who provided facilities for performing the 4 K EPR studies, and Dr. Stephane Ménage for technical assistance with these experiments.

[1] D. J. Kosman, M. J. Ettinger, R. E. Weiner, E. J. Massaro, *Arch. Biochem. Biophys.* **1974**, *165*, 456.
[2] M. M. Whittaker, J. W. Whittaker, *J. Biol. Chem.* **1988**, *263*, 6074.
[3] M. M. Whittaker, J. W. Whittaker, *J. Biol. Chem.* **1990**, *265*, 9610.
[4] N. Ito, S. E. V. Phillips, C. Stevens, Z. B. Ogel, M. J. McPherson, J. N. Keen, K. D. S. Yadav, P. J. Knowles, *Nature* **1991**, *350*, 87.
[5] G. T. Babcock, M. K. El-Deeb, P. O. Sandusky, M. M. Whittaker, J. W. Whittaker, *J. Am. Chem. Soc.* **1992**, *114*, 3727.
[6] N. Ito, S. E. V. Phillips, K. D. S. Yadav, P. F. Knowles, *J. Mol. Biol.* **1994**, *238*, 794.
[7] R. Sayle, E. F. Milner-White, *Trends Biochem. Sci.* **1995**, *20*, 374.
[8] J. W. Whittaker, *Metal Ions in Biological Systems* (Eds.: H. Sigel, A. Sigel), Marcel Dekker, New York, **1994**, vol. 30, pp. 315–360.
[9] J. W. Whittaker, in *Advances in Protein Chemistry* (Eds.: F. M. Richards, D. S. Eisenberg, J. Kuriyan), Academic Press, Elsevier, **2002**, vol. 60, pp. 1–49.
[10] J. W. Whittaker, *Chem. Rev.* **2003**, *103*, 2347.
[11] M. S. Rogers, D. M. Dooley, *Curr. Opin. Chem. Biol.* **2003**, *7*, 189.
[12] M. S. Rogers, A. J. Baron, M. J. McPherson, P. F. Knowles, D. M. Dooley, *J. Am. Chem. Soc.* **2000**, *122*, 990.
[13] M. S. Rogers, D. M. Dooley, *Curr. Opin. Chem. Biol.* **2003**, *7*, 189.
[14] S. J. Firbank, M. S. Rogers, C. M. Wilmot, D. M. Dooley, M. A. Halcrow, P. F. Knowles, M. J. McPherson, S. E. V. Phillips, *Proc. Natl. Acad. Sci. USA* **2001**, *98*, 12932.
[15] M. M. Whittaker, J. W. Whittaker, *J. Biol. Chem.* **2003**, *278*, 22090.
[16] N. Kitajima, K. Whang, Y. Moro-oka, A. Uchida, Y. Sasada, *J. Chem. Soc., Chem. Commun.* **1986**, 1504.
[17] Y. Wang, T. D. P. Stack, *J. Am. Chem. Soc.* **1996**, *118*, 13097.
[18] D. Zurita, I. Gautier-Luneau, S. Ménage, J. L. Pierre, E. Saint-Aman, *J. Biol. Inorg. Chem.* **1997**, *2*, 46.
[19] A. Sokolowski, H. Leutbecher, T. Weyhermüller, R. Schnepf, E. Bothe, E. Bill, P. Hildenbrandt, K. Wieghardt, *J. Biol. Inorg. Chem.* **1997**, *2*, 444.
[20] J. A. Halfen, B. A. Jazdzewski, S. Mahapatra, L. M. Berreau, E. C. Wilkinson, L. Que Jr, W. B. Tolman, *J. Am. Chem. Soc.* **1997**, *119*, 8217.
[21] E. Saint-Aman, S. Ménage, J. L. Pierre, E. Defrancq, G. Gellon, *New J. Chem.* **1998**, *22*, 393.
[22] Y. Wang, J. L. DuBois, B. Hedman, K. O. Hodgson, T. D. P. Stack, *Science* **1998**, *279*, 537.
[23] P. Chaudhuri, M. Hess, U. Flörke, K. Wieghardt, *Angew. Chem. Int. Ed.* **1998**, *37*, 2217.
[24] M. Vaidyanathan, R. Viswanathan, M. Palaniandavar, T. Balasubramanian, P. Prabhaharan, P. T. Muthiah, *Inorg. Chem.* **1998**, *37*, 6418.
[25] P. Chaudhuri, M. Hess, J. Müller, K. Hildenbrandt, E. Bill, T. Weyhermüller, K. Wieghardt, *J. Am. Chem. Soc.* **1999**, *121*, 9599.
[26] E. Bill, J. Müller, T. Weyhermüller, K. Wieghardt, *Inorg. Chem.* **1999**, *38*, 5795.
[27] P. Chaudhuri, M. Hess, T. Weyhermüller, K. Wieghardt, *Angew. Chem. Int. Ed.* **1999**, *38*, 1095.
[28] S. Itoh, M. Taki, S. Takayama, S. Nagatomo, T. Kitagawa, N. Sakurada, R. Arakawa, S. Fukuzumi, *Angew. Chem. Int. Ed.* **1999**, *38*, 2774.
[29] Y. Shimazaki, S. Huth, A. Odani, O. Yamauchi, *Angew. Chem. Int. Ed.* **2000**, *39*, 1666.
[30] M. Taki, H. Kumei, S. Nagatomo, T. Kitagawa, S. Itoh, S. Fukuzumi, *Inorg. Chim. Acta* **2000**, *300–302*, 622.

[31] C. Ochs, F. E. Hahn, R. Fröhlich, *Eur. J. Inorg. Chem.* **2001**, 2427.
[32] M. Vaidyannathan, M. Palaniandavar, R. S. Gopalan, *Inorg. Chim. Acta* **2001**, *324*, 241.
[33] L. Benisvy, A. J. Blake, D. Collison, E. S. Davies, C. D. Garner, E. J. L. McInnes, J. McMaster, G. Whittaker, C. Wilson, *Chem. Commun.* **2001**, 1824.
[34] M. Vaidyanathan, M. Palaniandavar, R. S. Gopalan, *Inorg. Chim. Acta* **2001**, *324*, 241.
[35] F. Thomas, G. Gellon, I. Gautier-Luneau, E. Saint-Aman, J.-L. Pierre, *Angew. Chem. Int. Ed.* **2002**, *41*, 3047.
[36] M. Vaidyanathan, M. Palaniandavar, R. S. Gopalan, *Ind. J. Chem. A* **2003**, *42*, 2210.
[37] G. Klein, J. M. Robertus, M. Watanabee, R. C. Pratt, T. D. P. Stack, *Chem. Commun.* **2003**, 630.
[38] R. C. Pratt, T. D. P. Stack, *J. Am. Chem. Soc.* **2003**, *125*, 8716.
[39] A. Neves, A. dos Anjos, A. J. Bortoluzzi, B. Szpoganicz, E. W. Schwingel, A. S. Mangrich, *Inorg. Chim. Acta* **2003**, *356*, 41.
[40] O. Seneque, M. Campion, B. Douziech, M. Giorgi, Y. Le Mest, O. Reinaud, *Dalton Trans.* **2003**, 4216.
[41] F. Thomas, O. Jarjayes, C. Duboc, C. Philouze, E. Saint-Aman, J.-L. Pierre, *Dalton Trans.* **2004**, 2662.
[42] R. C. Pratt, T. D. P. Stack, *Inorg. Chem.* **2004**, *43*, 8030.
[43] M. Taki, H. Hattori, T. Osako, S. Nagatomo, M. Shiro, T. Kitagawa, S. Itoh, *Inorg. Chim. Acta* **2004**, *357*, 3369.
[44] T. K. Paine, T. Weyhermüller, K. Wieghardt, P. Chaudhuri, *Dalton Trans.* **2004**, 2092.
[45] P. Chaudhuri, K. Wieghardt, T. Weyhermüller, T. K. Paine, S. Mukherjee, C. Mukherjee, *Biol. Chem.* **2005**, *386*, 1023.
[46] A. Dos Anjos, A. J. Bortoluzzi, R. E. H. M. B. Osorio, R. A. Peralta, G. R. Friedermann, A. S. Mangrich, A. Neves, *Inorg. Chem. Commun.* **2005**, *8*, 249.
[47] E. Zueva, P. H. Walton, J. E. McGrady, *Dalton Trans.* **2006**, 159.
[48] A. K. Nairn, S. J. Archibald, R. Bhalla, B. C. Gilbert, E. J. MacLean, S. J. Teat, P. H. Walton, *Dalton Trans.* **2006**, 172.
[49] A. Philibert, F. Thomas, C. Philouze, S. Hamman, E. Saint-Aman, J.-L. Pierre, *Chem. Eur. J.* **2003**, *9*, 3803.
[50] F. Michel, F. Thomas, S. Hamman, E. Saint-Aman, C. Bucher, J.-L. Pierre, *Chem. Eur. J.* **2004**, *10*, 4115.
[51] C. Xie, P. M. Lahti, *Tetrahedron Lett.* **1999**, *40*, 4305.
[52] L. Benisvy, A. J. Blake, D. Collison, E. S. Davies, C. D. Garner, E. J. L. McInnes, J. McMaster, G. Whittaker, C. Wilson, *Dalton Trans.* **2003**, 1975.
[53] C. G. Saysell, T. Barna, C. D. Borman, A. J. Baron, M. J. McPherson, A. G. Sykes, *J. Biol. Inorg. Chem.* **1997**, *2*, 702.
[54] F. Michel, F. Thomas, S. Hamman, C. Philouze, E. Saint-Aman, J.-L. Pierre, unpublished results.
[55] UV/Vis data [λ_{max} (nm) (ε {$M^{-1}cm^{-1}$})] for $[Cu^{II}(L^{H})]^{\cdot 2+}$: 401 (6560), 435 (4270), 694 (2420); for $[Cu^{II}(HL^{H})]^{\cdot 3+}$: 400 (11044), 435 (5200), 689 (3310). Complex $[Cu^{II}(L^{Me})]^{\cdot 2+}$ was too unstable to allow accurate ε values to be determined. The UV/Vis spectrum of $[Cu^{II}(L^{Me})]^{\cdot 2+}$ was found to be temperature-dependent (reversible process): the absorption bands at 395, 450 (shoulder) and 700 nm are only present at 298 K. Lowering the temperature to 233 K results in the disappearance of the lower energy absorption band, and changes in the 450 nm region. The same behavior is observed in the presence of excess pyridine (acting as an exogenous ligand, see ref.[4]). This is therefore not due to temperature dependent copper(II) coordination by the *p*-*N*-methylbenzimidazole moiety. Given the lack of additional information, more detailed discussion of this phenomenon would be premature.
[56] B. A. Jazdzewski, W. B. Tolman, *Coord. Chem. Rev.* **2000**, *200–202*, 633.
[57] S. Itoh, M. Taki, S. Fukuzumi, *Coord. Chem. Rev.* **2000**, *198*, 3.
[58] P. Chaudhuri, K. Wieghardt, *Prog. Inorg. Chem.* **2001**, *50*, 151.
[59] L. E. Kapinos, B. Song, H. Sigel, *Chem. Eur. J.* **1999**, *5*, 1794.
[60] R. Liu, K. Morokuma, A. M. Mebel, M. C. Lin, *J. Phys. Chem.* **1996**, *100*, 9314.
[61] A. Hinchliffe, R. E. Steinbank, M. A. Ali, *Theor. Chim. Acta* **1996**, *5*, 95.
[62] H. M. Chang, H. H. Jaffe, *Chem. Phys. Lett.* **1973**, *23*, 146.
[63] H. M. Chang, H. H. Jaffe, C. A. Masmandis, *J. Phys. Chem.* **1975**, *79*, 1118.
[64] J. Takahashi, T. Shida, *Bull. Chem. Soc. Jpn.* **1994**, *67*, 2038.
[65] J. Takahashi, T. Momose, T. Shida, *Bull. Chem. Soc. Jpn.* **1994**, *67*, 964.
[66] L. J. Johnston, N. Mathivanan, F. Negri, W. Siebrand, F. Zerbetto, *Can. J. Chem.* **1993**, *71*, 1655.
[67] J. G. Radziszewski, M. Gil, A. Gorski, J. Spanget-Larsen, J. Waluk, B. J. Mroz, *J. Chem. Phys.* **2001**, *115*, 9733.
[68] The thermodynamic feasibility of the reaction has been probed by recording the CV curve of $Cu(ClO_4)_2 \cdot 6H_2O$ in CH_3CN. The curve revealed a reduction peak at 0.32 V corresponding to the metal centered reduction wave of the hexaaquacopper(II). On the reverse scan, the oxidation peak is observed at a much higher value, 0.80 V, showing that a rearrangement in the metal coordination sphere occurs [this can be interpreted as the replacement of the water molecules by acetonitrile that stabilizes the copper(I) formal oxidation state]. The copper(II) ion is thus a strong oxidizer in acetonitrile, which can readily oxidize all of the copper(II) phenolate complexes ($[Cu^{II}(HL^{H})]^{2+}$ and $[Cu^{II}(HL^{Me})]^{2+}$) to the corresponding copper(II) phenoxyl radical complexes.
[69] When zero to one molar equiv. of copper(II) is added to acetonitrile solutions of HL^{H}, HL^{Me} and HL^{tBu}, in the presence of NEt_3, the phenolate copper(II) complexes are obtained, whichever ligand is used (the exogenous base NEt_3 scavenges the phenolic proton). Addition of one to two molar equiv. of copper(II) results in the disappearance of the phenolate copper(II) complex (characterized by its phenolate to copper CT transition). The UV/Vis spectra, after the addition of two molar equiv. of copper(II), exhibit absorption bands at around 400, 435 and 700 nm for HL^{H} and HL^{Me}, and 416 and 650 nm for HL^{tBu}. These features are similar to those of the electrogenerated $[Cu^{II}(L^{H})]^{\cdot 2+}$ and $[Cu^{II}(L^{tBu})]^{\cdot 2+}$ complexes, respectively. The copper(II) phenolate complexes are thus quantitatively oxidized by excess copper(II) to give the corresponding copper(II) phenoxyl complexes.
[70] C. Wright, A. G. Sykes, *J. Inorg. Biochem.* **2001**, *5*, 237.
[71] P. Nordlund, B.-M. Sjöberg, H. Eklund, *Nature* **1990**, *345*, 593.
[72] S. Un, M. Atta, M. Fontecave, A. W. Rutherford, *J. Am. Chem. Soc.* **1995**, *117*, 10713.
[73] P. P. Schmidt, K. K. Andersson, A.-L. Barra, L. Thelander, A. Graslünd, *J. Biol. Chem.* **1996**, *271*, 23615.
[74] P. J. Van Dam, J. P. Willems, P. P. Schmidt, S. Pötsch, A. L. Barra, W. R. Hagens, B. M. Hoffman, K. K. Andersson, A. Gräslund, *J. Am. Chem. Soc.* **1998**, *120*, 5080.
[75] B. A. Diner, D. A. Force, D. W. Randall, R. D. Britt, *Biochemistry* **1998**, *37*, 17931.
[76] J. Stubbe, W. A. van der Donk, *Chem. Rev.* **1998**, *98*, 705.
[77] P. Dorlet, A. W. Rutherford, S. Un, *Biochemistry* **2000**, *39*, 7826.
[78] Y.-N. Wang, L. A. Eriksson, *Int. J. Quantum Chem.* **2001**, *83*, 220.
[79] P. Faller, C. Goussias, A. W. Rutherford, S. Un, *Proc. Nat. Acad. Sc. USA* **2003**, *100*, 8732.
[80] T. Maki, Y. Araki, Y. Ishida, O. Onomura, Y. Matsumura, *J. Am. Chem. Soc.* **2001**, *123*, 3371.
[81] I. J. Rhile, J. M. Mayer, *J. Am. Chem. Soc.* **2004**, *126*, 12718.
[82] D. Kanamori, A. Furukawa, T.-A. Okamura, H. Yamamoto, N. Ueyama, *Org. Biomol. Chem.* **2005**, *3*, 1453.
[83] L. Benisvy, E. Bill, A. J. Blake, D. Collison, E. S. Davies, C. D. Garner, G. McArdle, E. J. L. McInnes, J. McMaster, S. H. K. Ross, C. Wilson, *Dalton Trans.* **2006**, 258.

Received: March 31, 2006
Published Online: August 3, 2006

